Investigation into the Catalytic Performance of Cu(II) Supported Graphene Quantum Dots Modified NiFe$_2$O$_4$ as a Proficient Nano-Catalyst in the Synthesis of Propargylasmines

Soudabeh Monajjemifar[1] · Farid Moeinpour[1] · Fatemeh S. Mohseni-Shahri[1]

Abstract

NiFe$_2$O$_4$ nanoparticles are modified by graphene quantum dots (GQDs) and utilized to stabilize the Cu(II) nanoparticles as a novel magnetically retrievable catalytic system (Cu(II)/GQDs/NiFe$_2$O$_4$) for green formation of propargylamines under solvent-free conditions. The various aldehydes/ketones, amines, and phenylacetylene were reacted at 100 °C in the presence of the catalyst to synthesize propargylamines. The prepared catalyst can be isolated assisted by an outer magnet and recovered for five courses without significant reduction in its efficiency. The as-prepared magnetic heterogeneous nanocomposite was characterized by UV–Vis, FT-IR, XRD, EDS, VSM, TEM, TGA and ICP. Performing the reactions in environmentally friendly and affordable conditions, the low catalyst percentage, high yield of products, short reaction times and easy workup are the merits of this protocol.

Graphic Abstract
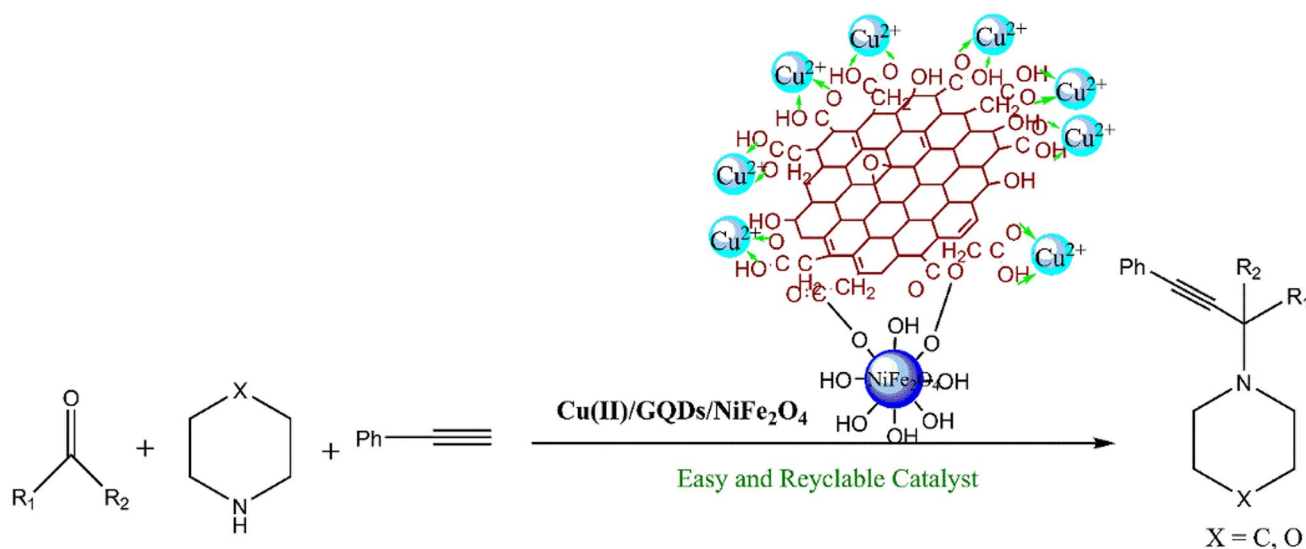
Keywords NiFe$_2$O$_4$ · Graphene quantum dots · Propargylamines · Solvent-free

✉ Farid Moeinpour
   fmoeinpour@iauba.ac.ir

[1] Department of Chemistry, Bandar Abbas Branch, Islamic
     Azad University, 7915893144 Bandar Abbas, Iran

1 Introduction

Graphene quantum dots (GQDs) are the zero-dimension nano-graphenes with special characteristics like small size, chemical inertness, photoluminescence, ease to be

functionalized with biomolecules and biocompatibility have received a lot of attention in the nanotechnology researches [1–3]. Nevertheless, the diverse uses of GQD, little consideration has been given for applying GQD as solid support or catalyst in the reactions [4–6]. Preparation of high-performing nano-catalysts for organic reactions is remain a major challenging task. To achieve greater specific area and more effective sites, nano-catalysts should be functionalized by activated moieties [7–9]. It is proved that the modification of the nano-catalyst with GQDs avoids the aggregation of fine particles and therefore enhances the active specific area for an effective catalytically reaction [8, 9]. Magnetic nanoparticles have been the focus of attention to researchers for consecutive years [10]. Many works have been published and also indicated that the importance of magnetic catalysts [11–14]. Among them, $NiFe_2O_4$ has been getting more consideration, owing to its strong coercive power, appropriate magnetic induction and high permanence [15]. Several researches verify the outlooks of using $NiFe_2O_4$ as an effective nano-catalyst [16–19]. The immobilization of nano-$NiFe_2O_4$ on GQDs will lead to a multi-purpose nano scaffold for efficient catalytic activity [20].

Propargylamines are very useful key components in the preparation of organic compounds, various natural products and pharmaceutical constituents. Due to the nucleophilic triple bond with a terminal acetylene hydrogen in propargylamines structure, in many cases they have high potential for diverse transformations. Three components linkage of amines, aldehydes, and alkynes, called A^3 coupling, is classified among the top ways to prepare propargylamines recently considered. Various transition metal and heterogeneous catalysts can carry out A^3 coupling reactions of terminal alkynes, amines and aldehydes by the way of C–H activating; for example, Magnetic CuO nanoparticles supported on graphene oxide [21], gold nanoparticles on ZnO [22], copper(I) complex immobilized on $Fe_3O_4@MCM-41$ nanoparticles, [23] iridium [24] and copper supported on $ZnAl_2O_4$, [25] under homogenous situations. In many cases, such methods for synthesis of propargylamines be affected by at least one limitation such as low-yielding, difficult reaction conditions, harsh working-up, prolonged reaction time and the utilization of high-cost and hazardous catalysts and solvents. For this reason, the development of high performance, clean, and eco-friendly strategies is still noteworthy and high demand. In continuation of our activities in propargylamine synthesis, [26, 27] herein, is discussed the preparation of Cu(II)/GQDs/$NiFe_2O_4$ by way of an easy co-sedimentation of $NiFe_2O_4$ nanoparticles on GQDs and its identification by diverse methods. The catalyst synthesis process is illustrated in Scheme 1. Upon full identification, the catalyst performance was investigated in preparation of propargylamines derivatives. The overall reaction is shown in Scheme 2.

2 Results and Discussion

The catalyst (Cu(II)/GQDs/$NiFe_2O_4$) was synthesized as specified by the procedure outlined in Scheme 1, by means of GQDs and $NiFe_2O_4$ nanoparticles produced in accord with literature [6, 15, 20, 28]. To verify synthesis of the nano-catalyst, it was completely identified using diverse methods comprising UV–vis and fluorescence spectroscopy, FT-IR spectroscopy, XRD, EDS, TEM, VSM and ICP spectroscopy.

The light-conducting characteristics of the prepared graphene quantum dots were examined by UV–Visible and fluorescence spectroscopy. The absorbing spectrum of graphene quantum dots does not give any peak as illustrated in Fig. 1a. The fluorescence spectra of graphene quantum dots could be observed in Fig. 1b. The graphene quantum dots were excited at wavelengths of 360, 380 and 400 nm and the proper fluorescence emission peaks were found at 454, 463 and 469 nm respectively. The emission peaks indicate a gentle red shift with a raising in the excitation wavelengths (360 – 400 nm). It has been observed that the color of the GQDs aqueous solution is weak yellow under visible light, but when excited by UV light at 365 nm, it seems blue, as indicated in the Fig. 1b. Changes in fluorescence intensity after the synthesis of GQDs/$NiFe_2O_4$ was also examined. The fluorescence spectra of GQDs/$NiFe_2O_4$, excited at 360, 380 and 400 nm is indicated in Fig. 2. The fluorescence emission peaks were found at 486, 483 and 480 nm respectively. It has been found that with increasing excitation wavelengths, a slight blue shift is observed in emission peaks. This differentiation in the fluorescence properties in comparison to the graphene quantum dots demonstrate the change in the chemical surface of the GQDs/$NiFe_2O_4$ implying a probable linkage of graphene quantum dots on the nickel ferrite nanoparticles, leading to a change in the surface characteristics of graphene quantum dots.

FT-IR spectroscopy was accomplished to validate the exterior framework of the nano-catalyst. The FT-IR spectrum has been displayed in Fig. 3 for Cu(II)/GQDs/$NiFe_2O_4$. The wide peak at 3362.97 cm^{-1} is assigned to the hydroxyl (O–H) bond, showing the absorption of water by the Cu(II)/GQDs/$NiFe_2O_4$. The bands located at 2981 cm^{-1} and 1450 cm^{-1} are related to the C-H bond vibrational stretching from remaining citric acid, implying the partial citric acid carbonization [29]. The peak located at 1001.35 cm^{-1} is related to the vibrational stretching of the C – O – C bond. The peaks located at 1415.34 and 1594.81 cm^{-1} would be the result of skeletal vibrations of aromatic rings in graphene quantum dots [30]. The presence of $NiFe_2O_4$ is validated by absorption bands located at 550.64 and 685.24 cm^{-1}, which are correlated to Ni–O
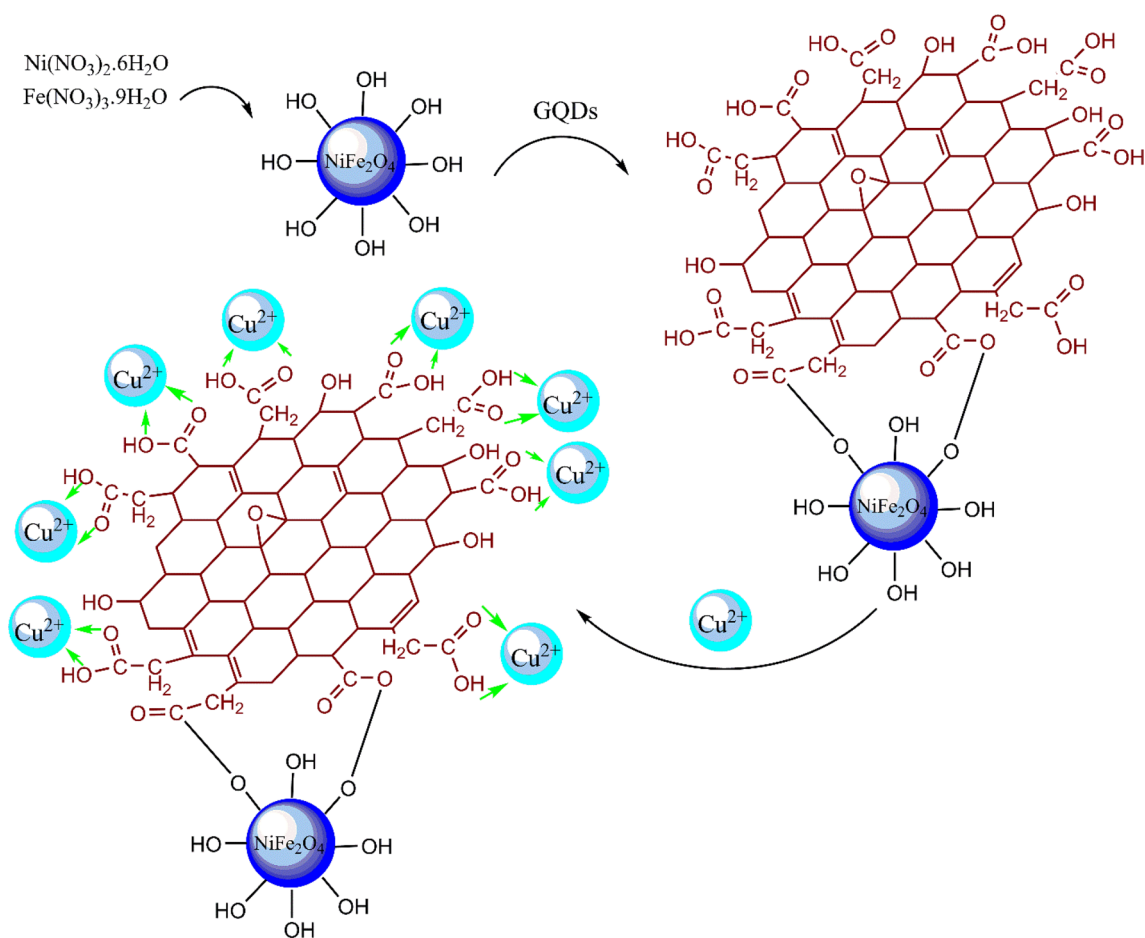
Scheme 1 Procedure for preparation of Cu(II)/GQDs/NiFe$_2$O$_4$

Scheme 2 Propargylamines synthesis catalyzed by Cu(II)/GQDs/NiFe$_2$O$_4$
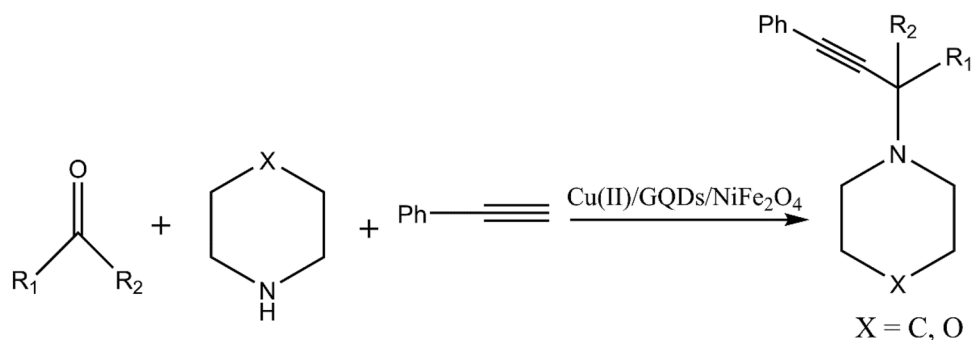
and Fe–O bonds vibrations, respectively [31]. The outcomes of this analysis confirm successful synthesis of magnetic nano-catalyst.

X-ray diffraction technique was employed to acquire information about the crystallinity of the nano-catalyst. XRD pattern of GQDs/NiFe$_2$O$_4$ was displayed in Fig. 4. The GQDs/NiFe$_2$O$_4$ diffraction pattern was agree well with the standard NiFe$_2$O$_4$ (JCPDS 10–0325) exhibits the important diffraction lines at 2θ = 17.15°, 30.59°, 35.76°, 37.30°, 43.43°, 53.84°, 57.34° and 63.01°, which may be attributed the (220), (311), (222), (400), (422), (511) and (440) planes of NiFe$_2$O$_4$ respectively. The diffraction peak of graphene quantum dots (004) (JCPDS 26–1080) is not recognizable, may have been due to their high dispersals and low crystallization degree of graphene quantum dots in GQDs/NiFe$_2$O$_4$ [15, 32].

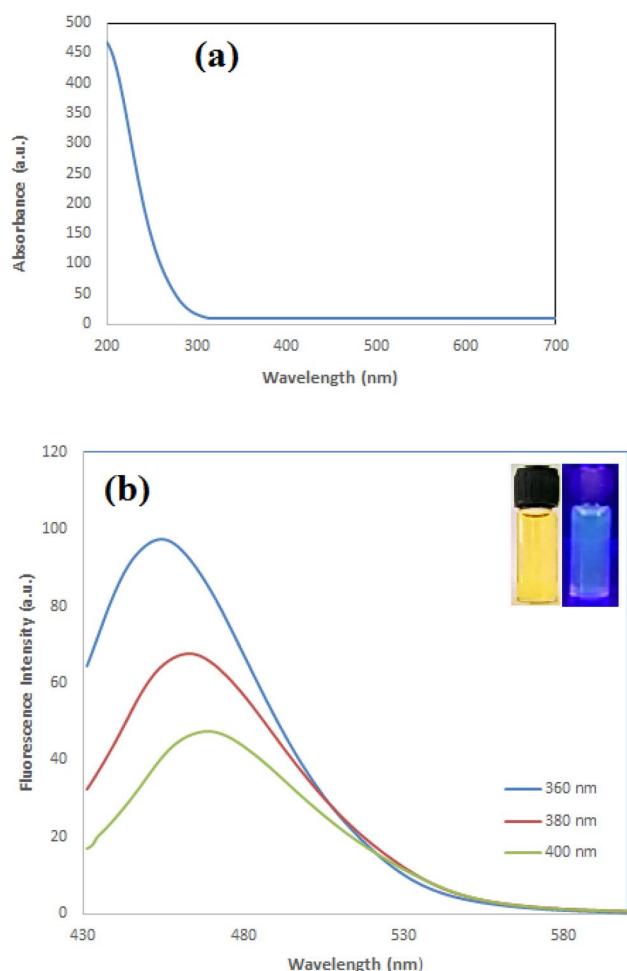The EDS was employed as an influential method to identify the chemical constitution of the produced nano-catalyst.

Fig. 1 a UV–Vis absorbance spectrum of GQDs, **b** Fluorescence spectra of GQDs. Inset shows pictures of GQDs solution taken under visible light (pale yellow) and 365 nm excitation (bluish-green)
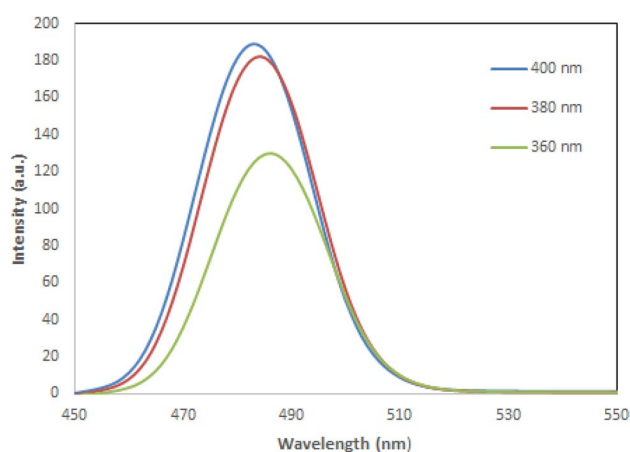

Fig. 2 Fluorescence spectra of Cu(II)/GQDs/NiFe$_2$O$_4$

The EDS analysis verifies the existence of envisaged elements comprising nickel, iron, oxygen, carbon and copper in the catalyst structure (Fig. 5).

The morphology and structural characteristics of the synthesized nano-catalyst was observed under TEM technique (Fig. 6). It is revealed that the darker region in Cu(II)/GQDs/NiFe$_2$O$_4$ image, is related to agglomeration of NiFe$_2$O$_4$ nanoparticles on GQDs. Also, the TEM micrograph of the nano-catalyst indicates that the mean sizes of Cu(II)/GQDs/NiFe$_2$O$_4$ nanoparticles are approximately not more than 40 nm.

The magnetic characteristic of Cu(II)/GQDs/NiFe$_2$O$_4$ was studied by VSM. As evidenced in Fig. 7, the value of the saturation magnetization of Cu(II)/GQDs/NiFe$_2$O$_4$ (60.82 emu. g^{-1}), almost equal to Fe$_3$O$_4$ nanoparticles (61.60 emu.g^{-1}) which indicates that the nano-catalyst has magnetic properties and their magnetic characteristics are so high that they could be isolated by a typical magnet.

The quantity of Cu loading onto the nano-catalyst was determined by the ICP technique which was obtained to be 0.94 mmol g^{-1}.

Thermogravimetric analysis (TGA) performed on GQDs/NiFe$_2$O$_4$ composite under N$_2$ atmosphere provides further evidence for GQDs encapsulation within NiFe$_2$O$_4$ cryast-allites (Fig. 8). For GQDs/ NiFe$_2$O$_4$ composites, about 30 wt% initial weight loss occurs at around 230–300 °C, corresponding to the decomposition of GQDs inside the NiFe$_2$O$_4$ crystals [33, 34]. So, we can assume that GQDs percent on GQD/NiFe$_2$O$_4$ is about 30%.

After validating the successful synthesis of nano-catalyst by various techniques, its catalytic capability was examined in the synthesis of propargylamines. To achieve this goal, benzaldehyde, phenylacetylene and morpholine were used as model substrates for optimizing the reaction elements including solvent, nano-catalyst amount and temperature. At the beginning, the above reaction was also conducted without and in the presence of various quantities of the nano-catalyst (Table 1). The outcomes revealed that the reaction did not progress in the absence of nano-catalyst even after 5 h (Table 1, entries 1–2). The reaction was not efficient in solvent conditions (Table 1, entries 3–8). Additionally, the influence of temperature was studied by performing the model reaction at various temperatures. Rising the temperature increases the reaction yield. This process occurred up to 100 °C (Table 1, entries 9–12). After that, increasing the temperature to 120 °C did not cause a significant increase in reaction yield Table 1, entry 13). Therefore, the optimum conditions were achieved when the model reaction was performed in solvent-free conditions in the presence of 0.03 g of nano-catalyst at 100 °C with 95% isolated yield (Table 1, entry 12). By enhancing the catalyst dosage until 0.05 g, no considerable change was obtained in the yield of the reaction (Table 1, entry 18). To illustrate the role of copper in
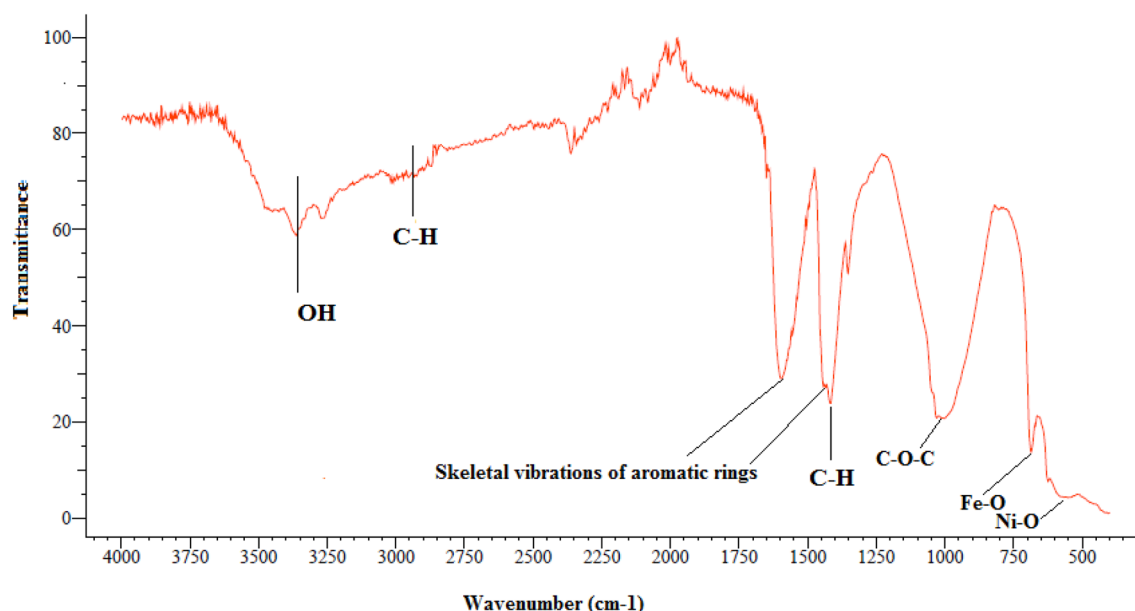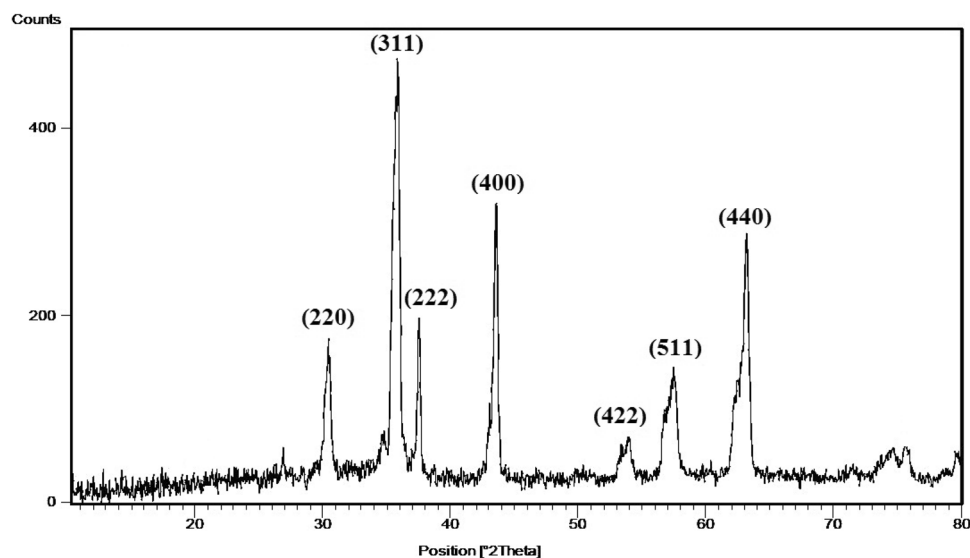
Fig. 3 FT-IR spectrum of Cu(II)/GQDs/NiFe$_2$O$_4$

Fig. 4 XRD pattern of GQDs/NiFe$_2$O$_4$

the reaction progress, the function of other components of the nano-catalyst like NiFe$_2$O$_4$, GQDs, and GQDs/NiFe$_2$O$_4$ was also examined in the reaction under optimal conditions. The outcomes are displayed in Table 1 (entries 19–21). As illustrated, no progress was detected in the model reaction when applying the other components of nano-catalyst in the absence of copper, verifying that the copper existence is vital for catalyzing the reaction. Also, the possibility of the model reaction in the presence of Cu(II)/NiFe$_2$O$_4$ was investigated. As can be seen in entry 21 of Table 1, the yield was 55%. This is less than the yield of the Cu(II)/GQDs/ NiFe$_2$O$_4$ catalyst. This could be due to insufficient Cu(II) supporting on the surface of nickel ferrite nanoparticles. The possibility of

the model reaction in the presence of Cu(II)/GQDs was not investigated. Assuming the reaction takes place, the catalyst has problems such as the difficulty of its separation from the reaction medium. We believe when we used Cu(II)/GQDs/ NiFe$_2$O$_4$, due to the nano features of GQDs and adsorption of the reactants on the surface of the catalyst, there was an increase in the local concentration of reactants around the active sites of the Cu(II)/GQDs/ NiFe$_2$O$_4$ which promoted the reaction effectively.

After creating optimal reaction conditions, the range of the reaction was expanded to diverse other kinds of reactants. In accord with the outcomes presented in Table 2, the electronic effects did not have affection on outcome of
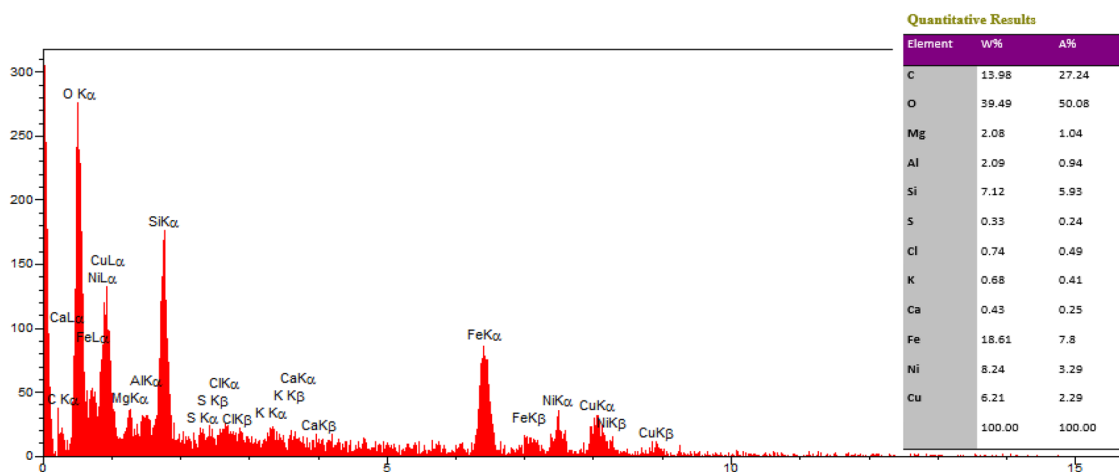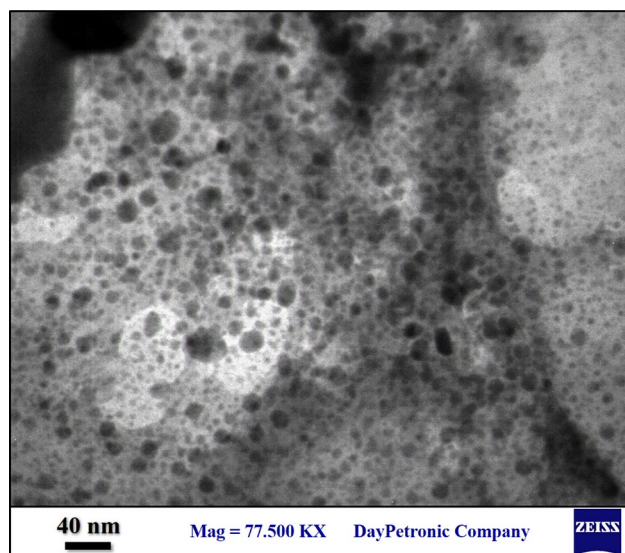
Fig. 5 EDS pattern of Cu(II)/GQDs/NiFe$_2$O$_4$

Fig. 6 TEM image of Cu(II)/GQDs/NiFe$_2$O$_4$

Fig. 7 Magnetization curve of Cu(II)/GQDs/NiFe$_2$O$_4$

the reaction. The electronic character of the substituents on the aromatic aldehydes had a noticeable effect on the final efficacy of the reaction. Substrates with electron-releasing groups (entries 3–12) all gave good transformations, while aryl aldehydes with electron-withdrawing groups (entries 13–16) needed prolonged times. The reaction capability of ketones is less than aldehydes and amongst ketones, cycloalkanones operates similar to benzaldehyde and its derivatives (entries 17–20).

In accord with literature [35], a plausible catalytic mechanism for the preparation of propargylamines by Cu(II)/GQDs/NiFe$_2$O$_4$ is suggested in Scheme 3. At first, alkyne is coordinated to Cu of the nano-catalyst. This interaction speeds up activation of the C – H bond and thereby facilitates the copper-alkylidine complex formation. In the next
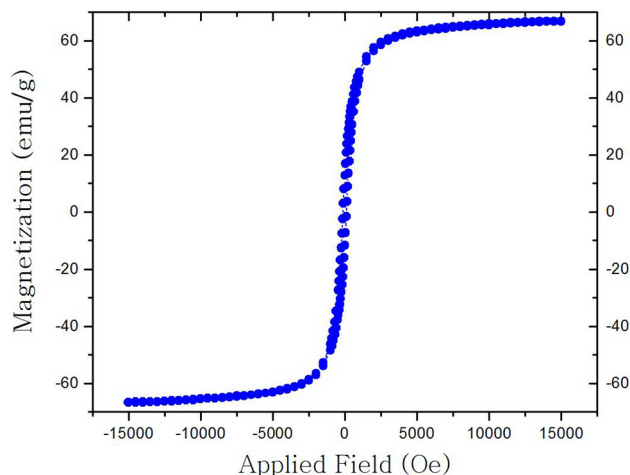
step, Cu – alkylidine intermediate reacts with iminium ion (produced on-site by the reaction of ketone or aldehyde and amine), to generate desirable propargylamine.

It is very important to recover and re-use catalysts from a commercial and industrial point of view as well as green chemistry. Thus, the reutilization of the catalyst [Cu(II)/GQDs/NiFe$_2$O$_4$] was examined in the sample reaction (benzaldehyde (1.0 mmol), morpholine (1.1 mmol), phenylacetylene (1.0 mmol) and catalyst (0.03 g, 2.8 mol%). For this goal, upon termination of the reaction, EtOAc (ethyl acetate) was added and the nano-catalyst was isolated by aid of an external magnet and reapplied in subsequent reactions. The outcomes revealed that the nano-catalyst could be successively retrieved five courses without any considerable reduction in its performance (Fig. 9 and Table 3).

To explore the leaking of copper, ICP study of the retrieved catalyst was additionally performed. In accord with
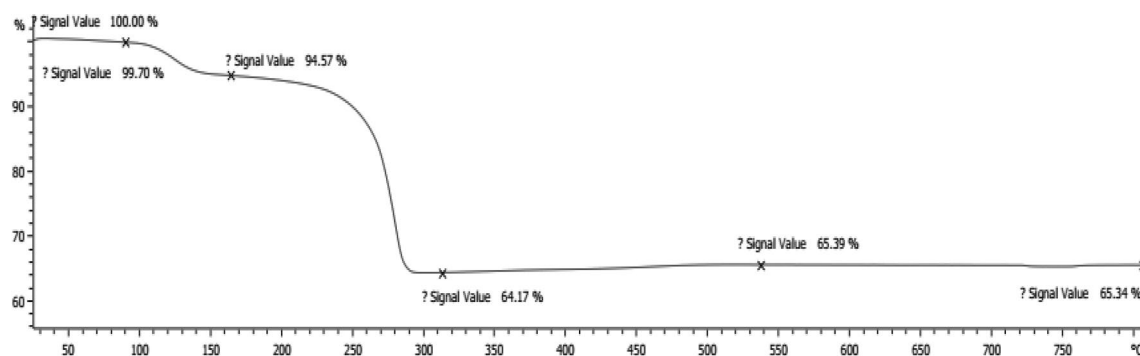
Fig. 8 TGA plot of GQDs/NiFe$_2$O$_4$

Table 1 Optimization of solvent, temperature, and nano-catalyst dosage

Entry	Condition	Catalyst (g, mol%)	Temp. (°C)	Time (h)	Yield (%)[a]
1	Solvent-free	–	Rt	5	None
2	Solvent-free	–	100	5	None
3	CH$_3$CN	(0.03, 2.8)	Reflux	5	10
4	EtOH	(0.03, 2.8)	Reflux	5	30
5	H$_2$O	(0.03, 2.8)	Reflux	5	40
6	Toluene	(0.03, 2.8)	Reflux	5	Trace
7	CH$_2$Cl$_2$	(0.03, 2.8)	Reflux	5	Trace
8	n-Hexane	(0.03, 2.8)	Reflux	5	Trace
9	Solvent-free (Cu(II)/GQDs/NiFe$_2$O$_4$)	(0.03, 2.8)	Rt	2	40
10	Solvent-free (Cu(II)/GQDs/NiFe$_2$O$_4$)	(0.03, 2.8)	60	0.5	60
11	Solvent-free (Cu(II)/GQDs/NiFe$_2$O$_4$)	(0.03, 2.8)	80	0.5	78
12	**Solvent-free (Cu(II)/GQDs/NiFe$_2$O$_4$)**	**(0.03, 2.8)**	**100**	**0.5**	**95**
13	Solvent-free (Cu(II)/GQDs/NiFe$_2$O$_4$)	(0.03, 2.8)	120	0.5	97
14	Solvent-free (Cu(II)/GQDs/NiFe$_2$O$_4$)	(0.01, 0.9)	100	0.5	80
15	Solvent-free (Cu(II)/GQDs/NiFe$_2$O$_4$)	(0.02, 1.9)	100	0.5	90
17	Solvent-free (Cu(II)/GQDs/NiFe$_2$O$_4$)	(0.04, 3.8)	100	0.5	97
18	Solvent-free (Cu(II)/GQDs/NiFe$_2$O$_4$)	(0.05, 4.7)	100	0.5	97
19	Solvent-free (NiFe$_2$O$_4$)	0.03	100	1	None
20	Solvent-free (GQDs)	0.03	100	1	None
21	Solvent-free (GQDs/NiFe$_2$O$_4$)	0.03	100	1	None
22	Solvent-free (Cu(II)/NiFe$_2$O$_4$)	0.03	100	1	55

Reaction conditions: benzaldehyde (1.0 mmol), morpholine (1.1 mmol), phenylacetylene (1.0 mmol)
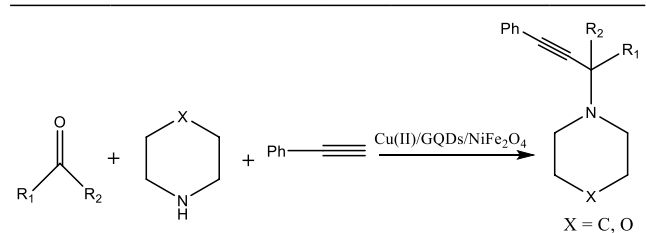
[a]On the basis of isolated yield

the acquired outcomes, no considerable reduction was monitored in the Cu quantity. The Cu amount in the new nano-catalyst and the recovered one was 0.94 and 0.91 mmol g^{-1}, respectively, which revealed the amount of leached Cu for this nano-catalyst is very slight. XRD pattern of the recovered catalyst indicated in Fig. 10. From the obtained XRD pattern obviously exhibited the fresh and used form of catalyst structure approximately similar. Thus, emphasizing no considerable changes happened during the course of reaction.

To validate the advantage of the present research, application of Cu(II)/GQDs/NiFe$_2$O$_4$ in producing of propargylamines (phenylacetylene, benzaldehyde and morpholine) in comparison with other formerly reported heterogeneous catalysts is presented in Table 4. In accordance with the results, the introduced catalyst indicates more adequate catalytic performance under environmentally friendly and affordable conditions.

Given that most of the products have been previously synthesized, reported and identified, characterization of the synthesized products is restricted to ^{1}HNMR and ^{13}CNMR spectra for some products.

Table 2 Synthesis of propargylamine derivatives in the presence of catalyst

Entry	R_1, R_2	X	Time (min.)	Yield[a] (%)
1	Ph, H	O	30	95
2	Ph, H	C	30	96
3	4-MeC$_6$H$_4$, H	O	45	95
4	Cl, H	O	30	90
5	4-OMeC$_6$H$_4$, H	O	45	98
6	4-(NMe$_2$)C$_6$H$_4$, H	O	45	86
7	2-OHC$_6$H$_4$, H	O	30	95
8	4-MeC$_6$H$_4$, H	C	45	91
9	Cl, H	C	30	91
10	4-OMeC$_6$H$_4$, H	C	45	95
11	4-(NMe$_2$)C$_6$H$_4$, H	C	45	87
12	2-OHC$_6$H$_4$, H	C	140	97
13	4-NO$_2$C$_6$H$_4$, H	O	140	75
14	4-NO$_2$C$_6$H$_4$, H	C	140	78
15	4-CNC$_6$H$_4$, H	O	125	92
16	4-CNC$_6$H$_4$, H	C	125	87
17	Cyclopentanone	O	30	95
18	Cyclohexanone	O	30	95
19	Cyclopentanone	C	30	98
20	Cyclohexanone	C	30	94
21	2-Thiophenyl, H	O	200	86

Aldehyde or ketone (1 mmol), secondary amine (1.1 mmol), phenylacetylene (1 mmol), catalyst (0.03 g), 100 °C

[a]based on isolated yields

3 Conclusions

We have successfully synthesized a copper heterogeneous catalyst on graphene quantum dots/NiFe$_2$O$_4$ nano-magnetic particles as a very stable and recoverable nano-catalyst for the green production of propargylamines derivatives under solvent-less conditions. The proposed reaction, in which the designed Cu(II)/GQDs/NiFe$_2$O$_4$ as a recoverable catalyst, consistent with the principles of green chemistry owing to the following properties: no toxicity, great durability, recovery capability, shorter times of reaction, and good to excellent products yields. Above all others, the nano-catalyst could be recovered five runs without any failure in its productivity. So, the prepared nano-catalyst is might be useful in related industries.

4 Experimental

Citric acid, sodium hydroxide, nickel nitrate, Fe(III) nitrate and Cu(II) acetate were purchased from Sigma. UV–vis absorption investigations were conducted by Hach DR 6000 UV–visible spectrophotometer. Fluorescence examinations were done on Jasco FP-6200 spectrofluorophotometer (Hitachi Japan). The phase crystallinity of the prepared nano-catalyst was studied by a diffractometer at wavelength of 1.540 Å (Philips Company). Transmission electron microscopy (TEM) picture were captured by means of Zeiss electron microscope, LEO 912AB (120 kV), Germany. Fourier transform infrared (FT-IR) spectra were recorded on a Bruker model 470 spectrophotometer. Magnetic characteristics were registered on a vibrating sample magnetometer apparatus (VSM, LDJ9600) at environment temperature. EDS spectroscopy study were conducted with 133 eV resolution (model 7353, Oxford Instruments, UK). Copper determination was carried out by inductively coupled plasma (ICP) technique on a Varian VISTA-PRO. NMR spectra were registered in CDCl$_3$ on a Bruker Advance 300 MHz instrument.

4.1 Synthesis of NiFe$_2$O$_4$ Nanoparticles

Egg white (60 mL) was added to distilled water (40 ml) and was shaken hard to perfectly mix. Subsequently, 2.9081 g (10 mmol) of nickel nitrate hexahydrate and 8.0800 g (20 mmol) of Fe(III) nitrate nonahydrate were dissolved in the above solution and was stirred hard at ordinary-temperature for 2 h. Then, whilst the mixture was agitated, it was warmed to 80 °C until dried. The consequent powder was grinded and then heated at 700 °C for 3 h [15].

4.2 Synthesis of Graphene Quantum Dots (GQDs)

GQDs were made from thermally decomposed citric acid [28]. concisely, citric acid (0.2 g, 1.0 mmol) was melted and heated at 200° C for 5 min. Then, the subsequent yellowish liquid was added progressively into 20 mL of 0.25 M NaOH solution. Thereafter, the GQDs solution was dialyzed in a 1 kDa dialysis bag for 24 h (dialysate was exchanged every 8 h) to eliminate the unreacted chemicals. The produced graphene quantum dots solution was maintained in 4 °C.

4.3 Synthesis of GQDs/NiFe$_2$O$_4$

NiFe$_2$O$_4$ nanoparticles, 1 g were dispersed sonochemically in water (5 mL) for 15 min. Afterwards, the GQDs suspension (20 mL, final concentration, 1.125 mg.L^{-1}) was added to the flask comprising the NiFe$_2$O$_4$ nanoparticles and

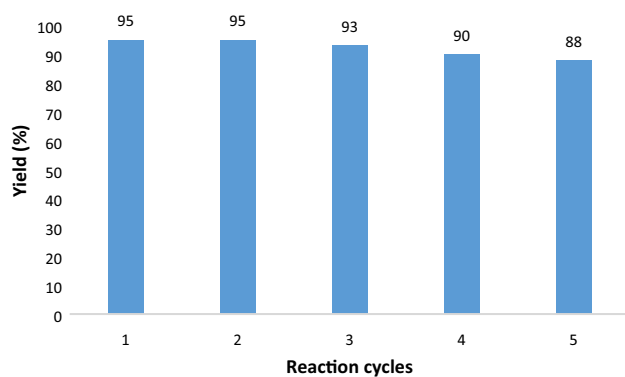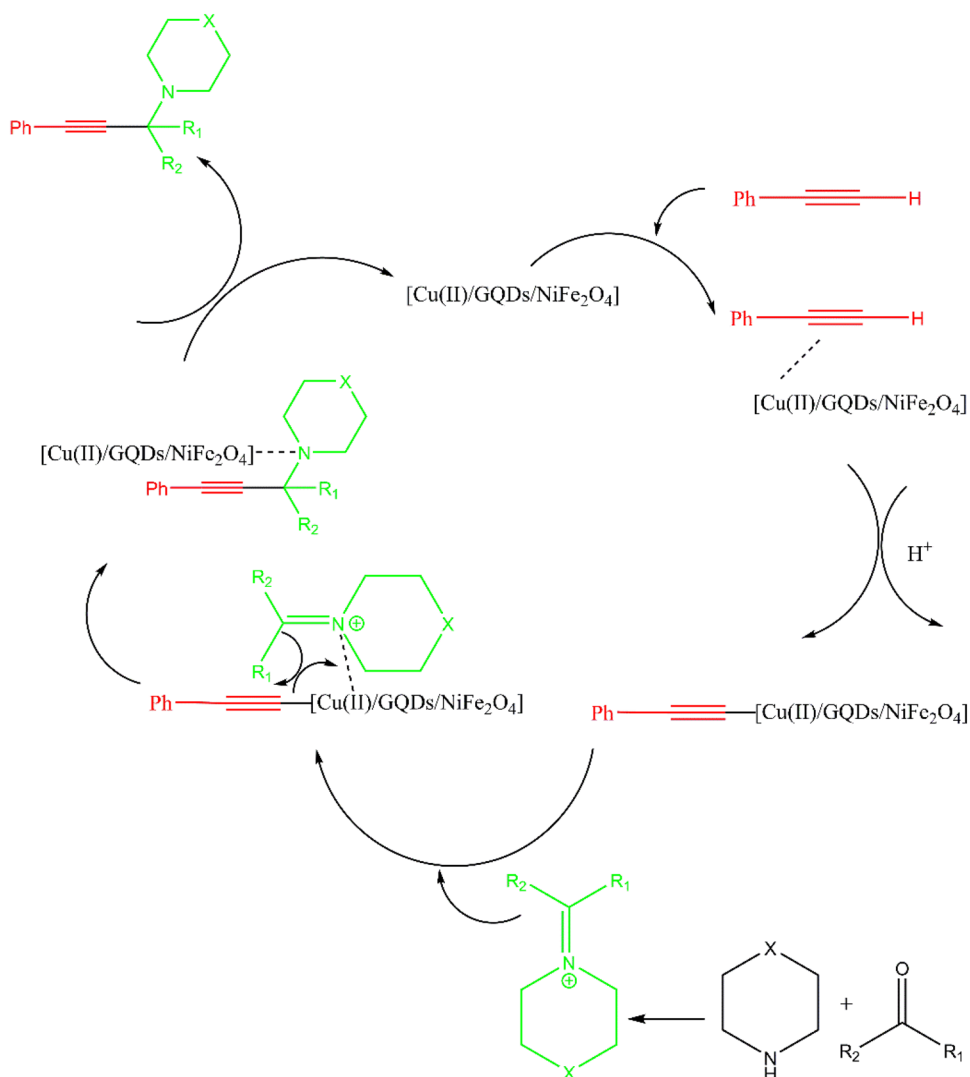**Scheme 3** Proposed mechanism for the preparation of propargylamines in the presence of Cu(II)/GQDs/NiFe$_2$O$_4$

**Fig. 9** Reusability of Cu(II)/GQDs/NiFe$_2$O$_4$ in the model reaction

Table 3 TON and TOF values for the reusability of Cu(II)/GQDs/NiFe$_2$O$_4$ in the model reaction

Reaction cycle	Yield (%)	TON[a]	TOF[b] (min^{-1})
1	95	33.93	1.13
2	95	33.93	1.13
3	93	33.21	1.14
4	90	32.86	1.11
5	88	31.43	1.05

[a]Turnover number

[b]Turnover frequency = TON/time, time = 30 min

the resulting mixture was shaken for 48 h at 60 °C. The produced GQDs modified NiFe$_2$O$_4$ was isolated through the use of a magnet and was washed with distilled water

Fig. 10 XRD pattern of the used catalyst
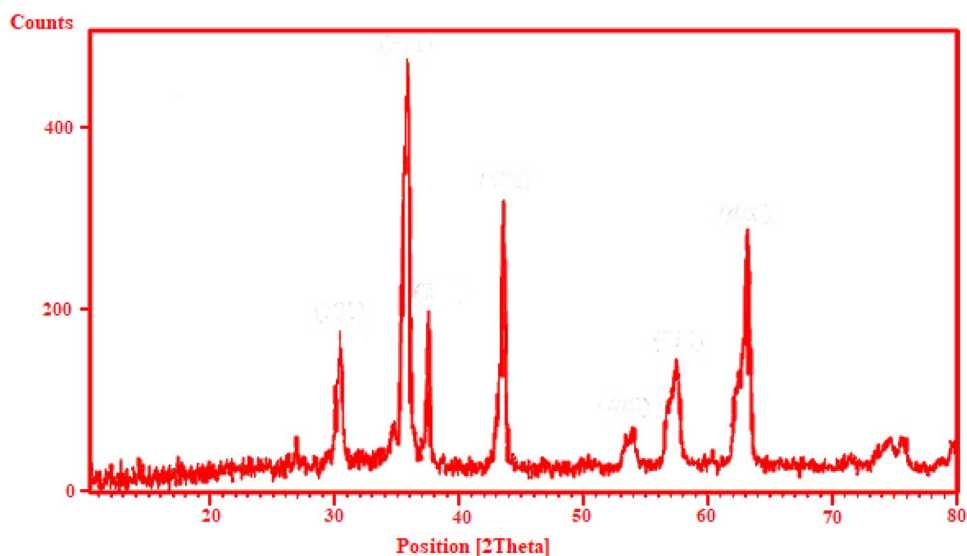
Table 4 Comparability of Cu(II)/GQDs/NiFe$_2$O$_4$ nano-catalyst with different heterogeneous catalytic systems in preparation of propargylamines

Entry	Catalyst	Solvent	Temp. (°C)	Time (h)	Yield (%)[a]	References
1	CuNPs/TiO$_2$	Solvent-free	80	7	98	[36]
2	Zn(II)/HAP/Fe$_3$O$_4$	Solvent-free	110	3	95	[37]
3	ZnCl$_2$-TiO$_2$	Solvent-free	100	6	97	[38]
4	Au-MCM-41	H$_2$O	80	24	80	[39]
5	GO-Cu	H$_2$O	100	15	83	[40]
6	Au-Mont	Toluene	100	3	91	[41]
7	Cu(II)/GQDs/NiFe$_2$O$_4$	Solvent-free	100	1	95	This study

(3×20 mL) and ethanol (3×20 mL) and finally dried under low pressure [20].

4.4 Synthesis of Cu(II)/GQDs/NiFe$_2$O$_4$

GQDs/NiFe$_2$O$_4$ (0.5 g) was dispersed in acetone (25 mL) at ordinary temperature for 30 min. Afterwards, 0.1 mmol copper(II) acetate (0.018 g) was added gently to the flask comprising GQDs/NiFe$_2$O$_4$ nanocomposite. The consequent mixture was mechanically shaken for 48 h at ambient temperature. Then, the solid was isolated with the aid of a magnet, washed with water (3×25 mL) and ethanol (3×25 mL) and finally dried at 60 °C overnight [6].

4.5 Synthetic Typical Manner for Synthesis of Propargylamines

Cu(II)/GQDs/NiFe$_2$O$_4$ catalyst (0.03 g, 2.8 mol%) was added to a solution comprising aldehydes or ketones (1.0 mmol), phenylacetylene (1.0 mmol) and secondary amines (1.1 mmol) in a rounded bottom flask was heated at 100 °C under solvent-free condition for proper reaction time (30—200 min.). The proceed of the reaction was controlled using thin layer chromatography, whenever the reaction was completed, the reaction mixture was diluted with hot ethanol and the nano-catalyst was isolated with the aid of a magnet, washed with acetone and then dried on a night to be ready to react again. The products were extracted from the reaction mixtures with ethyl acetate and water consecutively. The organic layer was dried over anhydrate sodium sulfate and after that, evaporated to separate the solvent. The remaining part was isolated by column chromatography utilizing n-hexane–ethyl acetate (5:1) as elution solvent to provide pure corresponding propargylamines derivatives. The products were recognized by ^{13}C-NMR and ^{1}H-NMR spectroscopy.

4.6 Spectral Data for Chosen Derivatives

4.6.1 4-(1, 3-diphenylprop-2-yn-1-yl)morpholine (Table 2, entry 1)

^{1}HNMR (300 MHz, CDCl$_3$): δ = 2.68 (4H, t, J = 4.35), 3.77-3.82 (4H, m), 4.84 (1H, s), 7.39-7.71 (10H, m); ^{13}C NMR (75 Hz, CDCl$_3$): δ = 50, 62.08, 67.21, 85.08, 88.55,

123.02,127.82, 128.27, 128.32, 128.37, 128.65, 131.84, 137.85.

4.6.2 1-(1,3-Diphenylprop-2-yn-1-yl)piperidine (Table 2, entry 2)

^{1}HNMR (300 MHz, CDCl$_3$): δ = 1.57–1.61 (2H, m), 1.64–1.78 (4H, m), 2.71 (4H, t, J = 5.26), 4.95 (1H, s), 7.38–7.46 (6H, m, 2-Ar), 7.63–7.66 (2H, m, Ar), 7.77–7.79(2H, m, Ar); ^{13}CNMR (75 Hz, CDCl$_3$): δ = 24.56, 26.27, 50.79, 62.45, 84.12, 88.02, 123.43,127.61, 128.19, 128.38, 128.67, 131.93, 138.62.

4.6.3 4-(1-(4-Methoxyphenyl)-3-phenylprop-2-yn-1-l) morpholine (Table 2, entry 5)

^{1}HNMR (300 MHz, CDCl$_3$): δ = 2.67–2.71 (4H, m), 3.77–3.78 (4H, m), 4.78 (1H, s), 6.95–6.98 (d, 2H, J = 8.7, Ar), 7.35–7.38 (2H, m, J = 6.4, Ar), 7.58–7.63 (d, 2H, J = 8.2, Ar); ^{13}C NMR (75 Hz, CDCl$_3$): δ = 49.88, 55.31, 61.48, 67.21, 85.47, 88.34, 113.63, 123.09, 128.28, 128.37, 129.77, 129.93,131.86, 159.28.

4.6.4 1-(3-Phenyl-1-(p-tolyl)prop-2-yn-1-yl)piperidine (Table 2, entry 8)

^{1}HNMR (300 MHz, CDCl$_3$): δ = 1.57–1.64 (2H, m), 1.65–1.76 (4H, m), 2.47 (3H, s), 2.66 (4H, t, J = 4.9), 7.28 (2H, d, J = 8.1), 7.38–7.44 (3H, m), 7.60–7.63 (2H, m), 7.65 (2H, d, J = 8.1); ^{13}CNMR (75 Hz, CDCl$_3$): δ = 21.25, 24.57, 29.27, 50.72, 62.23, 86.47, 87.72, 123.51, 128.12, 128.37, 128.59, 128.87, 131.92, 135.66, 137.14.

4.6.5 4-(1-(Phenylethynyl)cyclohexyl)morpholine (Table 2, entry 18)

^{1}HNMR (300 MHz, CDCl$_3$): δ = 1.27–1.78 (8H, m), 2.04–2.08 (3H, m), 2.77 (4H, t, J = 4.8 Hz), 3.81 (4H, t, J = 4.8 Hz), 7.31–7.47 (5H, m); ^{13}CNMR (75 Hz, CDCl$_3$): δ = 22.78, 25.71, 29.34, 35.46, 46.67, 58.95, 67.50, 86.53, 89.78, 123.44, 128.23, 131.74.

References

1. Li Y, Hu Y, Zhao Y, Shi G, Deng L, Hou Y, Qu L (2011) Adv Mater 23:776–780
2. Shen J, Zhu Y, Yang X, Li C (2012) Chem Comm 48:3686–3699
3. Li L, Wu G, Yang G, Peng J, Zhao J, Zhu JJ (2013) Nanoscale 5:4015–4039
4. Du Y, Guo S (2016) Nanoscale 8:2532–2543
5. Jin H, Huang H, He Y, Feng X, Wang S, Dai L, Wang J (2015) J Am Chem Soc 137:7588–7591
6. Gholinejad M, Ahmadi J, Nájera C, Seyedhamzeh M, Zareh F, Kompany-Zareh M (2017) Chem Cat Chem 9:1442–1449
7. Hu E, Yu XY, Chen F, Wu Y, Hu Y, Lou XW (2018) Adv Energy Mater 8:1702476. https://doi.org/10.1002/aenm.201702476
8. Koli PB, Kapadnis KH, Deshpande UG, Patil MR (2018) J Nanostruct Chem 8:453–463
9. Pirhaji JZ, Moeinpour F, Dehabadi AM, Ardakani SAY (2019) J Mol Liq 112345.
10. Narayanan S, Sathy BN, Mony U, Koyakutty M, Nair SV, Menon D (2011) ACS Appl Mater Interf 4:251–260
11. Omidvar-Hosseini F, Moeinpour F (2016) J Water Reuse Desalin 6:562–573
12. Javid A, Khojastehnezhad A, Eshghi H, Moeinpour F, Bamoharram FF, Ebrahimi J (2016) Org Prep Proc Int 48:377–384
13. Bronstein LM (2015) Chem Cat Chem 7:1058–1060
14. Khakzad Siuki MM, Bakavoli M, Eshghi H (2019) Appl Organomet Chem 33:e4774
15. Maensiri S, Masingboon C, Boonchom B, Seraphin S (2007) Script Mater 56:797–800
16. Khojastehnezhad A, Moeinpour F, Javid A (2019) Polycycl Aromat Comp 39:404–412
17. Rahimizadeh M, Seyedi SM, Abbasi M, Eshghi H, Khojastehnezhad A, Moeinpour F, Bakavoli M (2015) J Iran Chem Soc 12:839–844
18. Shylesh S, Schünemann V, Thiel WR (2010) Magnetically separable nanocatalysts: bridges between homogeneous and heterogeneous catalysis. Angew Chem Int Ed 49:3428–3459
19. Pourshojaei Y, Zolala F, Eskandari K, Talebi M, Morsali L, Amiri M, Khodadadi A, Shamsimeymandi R, Faghih-Mirzaei E, Asadipour A (2020) J Nanosci Nanotechnol 20:3206–3216
20. Ramachandran S, Sathishkumar M, Kothurkar NK, Senthilkumar R (2018) IOP Conference Series: Materials Science and Engineering. IOP Publishing 310:012139
21. Mirabedini M, Motamedi E, Kassaee MZ (2015) Chin Chem Lett 26:1085–1090
22. González-Béjar M, Peters K, Hallett-Tapley GL, Grenier M, Scaiano JC (2003) Chem Comm 49:1732–1734
23. Moaddeli A, Abdollahi-Alibeik M (2018) J Porous Mater 25:147–159
24. Fischer C, Carreira EM (2001) Org Lett 3:4319–4321
25. Mandlimath TR, Sathiyanarayanan KI (2016) RSC Adv 6:3117–3125
26. Khojastehnezhad A, Bakavoli M, Javid A, Siuki MMK, Moeinpour F (2019) Catal Lett 149:713–722
27. Khakzad Siuki MM, Bakavoli M, Eshghi H (2018) Appl Organomet Chem 32:e4290
28. Benítez-Martínez S, Valcárcel M (2015) Anal Chim Act 896:78–84
29. Dong Y, Shao J, Chen C, Li H, Wang R, Chi Y, Lin X, Chen G (2012) Carbon 50:4738–4743
30. Teymourinia H, Salavati-Niasari M, Amiri O, Safardoust-Hojaghan H (2017) J Mol Liq 242:447–455
31. Yamaura M, Camilo R, Sampaio L, Macedo M, Nakamura M, Toma H (2004) J Magn Magn Mater 279:210–217
32. Alvand M, Shemirani F (2017) Microchim Acta 184:1621–1629
33. Biswal BP, Shinde DB, Pillai VK, Banerjee R (2013) Nanoscale 5:10556–10561
34. Hu T, Chu X, Gao F, Dong Y, Sun W, Bai L (2016) J Solid State Chem 237:248–291
35. Albaladejo MJ, Alonso F, Moglie Y, Yus M (2012) Eur J Org Chem 2012:3093–3104

36. Perumgani PC, Keesara S, Parvathaneni S, Mandapati MR (2016) New J Chem 40:5113–5120

37. Zarei Z, Akhlaghinia B (2016) RSC Adv 6:106473–106484

38. Bankar DB, Hawaldar RR, Arbuj SS, Moulavi MH, Shinde ST, Takle SP, Shinde MD, Amalnerkar DP, Kanade KG (2019) RSC Adv 9:32735–32743

39. Feiz A, Bazgir A (2016) Catal Comm 73:88–92

40. Kumari S, Shekhar A, Pathak DD (2016) RSC Adv 6:15340–15344

41. Borah BJ, Borah SJ, Saikia K, Dutta DK (2014) Catal Sci Technol 4:4001–4009